



Proceedings of the Sixth International Conference on  
Railway Technology: Research, Development and Maintenance  
Edited by: J. Pombo  
Civil-Comp Conferences, Volume 7, Paper 11.3  
Civil-Comp Press, Edinburgh, United Kingdom, 2024  
ISSN: 2753-3239, doi: 10.4203/ccc.7.11.3  
©Civil-Comp Ltd, Edinburgh, UK, 2024

# **Evaluation of Site Amplification Factors on the Seafloor for Use in Earthquake Early Warning for Railways Based on Accumulated Seismic Data**

**H. Miyakoshi, K. Kinoshita, R. Nakayama, T. Keyaki  
and K. Kato**

**Research and Development Center for JR East Group,  
East Japan Railway Company  
Saitama, Japan**

## **Abstract**

Since November 2017, the earthquake early warning for Shinkansen uses ocean bottom seismometer, and an alarm is issued when the ocean bottom seismometer exceeds the threshold. The threshold is set by multiplying the reference value that changes with distance from Shinkansen line to seismometer due to attenuation and the site amplification factor of seismic motion due to soft sedimentary layer beneath the seafloor. However, the site amplification factor is poor accuracy, because that factor is set to the average value at all observation points since there was little observation data when the ocean bottom seismometer was introduced. Therefore, in this study, we proposed a method to set precise site amplification factor according to the installation environment of the ocean bottom seismometer by utilizing the accumulated seismic data observed by the ocean bottom seismometer.

**Keywords:** earthquake, Shinkansen, earthquake early warning, ocean bottom seismometer, site amplification factor, attenuation relation, acceleration, sediment thickness.

## **1 Introduction**

East Japan Railway Company (JR East) has introduced the early earthquake warning (EEW) system that immediately stops Shinkansen trains based on the earthquake information from seismometers installed along railroads and coastlines,

etc., in order to ensure the safety of running trains during earthquakes [1]. After the 2011 off the Pacific coast of Tohoku Earthquake, the National Research Institute for Earth Science and Disaster Resilience (NIED) has installed the Seafloor observation network for earthquakes and tsunamis along the Japan Trench (S-net) [2, 3]. In Figure 1, locations of the seismometers of JR East’s EEW system for Shinkansen and those of the observatories and the land stations of S-net are shown. Ocean bottom seismometers (OBSs) in the observatories of S-net can detect earthquakes occurring near the Japan Trench earlier than seismometers installed on the land. JR East, therefore, began using seismic information observed by the OBSs of S-net for its EEW system for Shinkansen from November 2017 [4, 5].

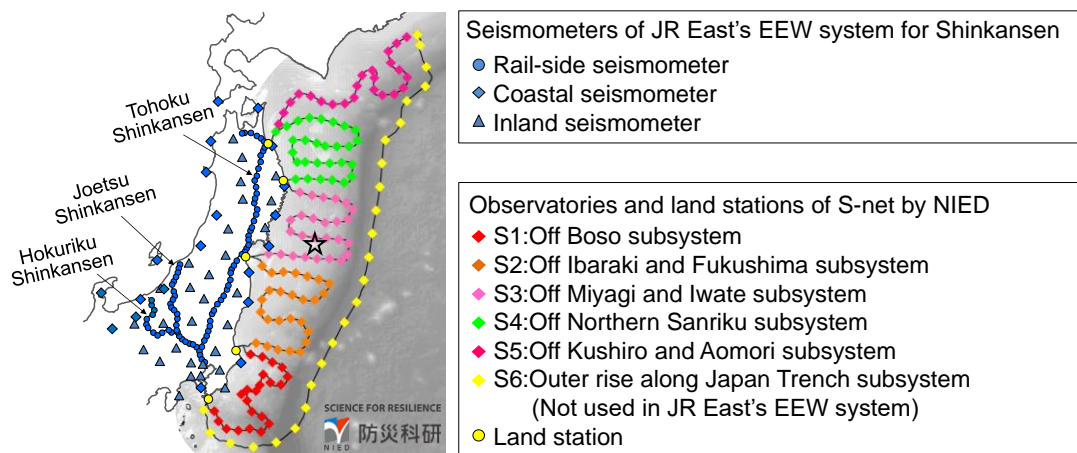


Figure 1: Locations of seismometers of JR East’s EEW system for Shinkansen and those of observatories and land stations of S-net by NIED (Modifying part of the OBS map provided by NIED).

The EEWs using the OBSs of S-net are issued when the earthquake motion intensity observed by the OBSs exceeds certain thresholds. As of 2017, it was necessary to establish a common threshold for all the OBSs due to few observation records. As long time has passed from starting the observation of S-net and the data have accumulated, we reconsider the threshold for each OBS of S-net in this study.

## 2 Threshold of EEW for Shinkansen using OBS

The EEWs for JR East’s Shinkansen using the OBSs of S-net are types of warning called “S-wave warning,” which is issued when acceleration observed by seismic stations exceeds a predetermined threshold [6]. The acceleration is called “JR filtered acceleration” and subjected to the band-pass filter (pass band 0.05-5 Hz, defined by the Japan National Railway at the time) to better grasp correlation with the damage of railway structures [7]. The threshold is established as the value obtained by multiplying the standard value according to the distance between the OBS and the railway line by the site amplification factor by the sediment beneath the seafloor [4, 5]. In Figure 2, the conceptual figure showing the conditions for setting a threshold for an OBS is shown. The standard value is determined as the JR filtered acceleration

at the OBS when the JR filtered acceleration at the railway line is 80 cm/s<sup>2</sup> in the subduction-zone earthquake that occurs around the OBS. Both JR filtered acceleration at the railway line and that at the OBS are estimated using the attenuation relation of JR filtered acceleration, which is expressed by the following equation [8].

$$\log_{10}(JRPGA) = 0.54634M_j + 0.0058D - 0.00332X - 0.01746 - \log_{10}(X + 0.00492 \cdot 10^{0.5M_j}) \quad (1)$$

where *JRPGA* is JR filtered acceleration, *M<sub>j</sub>* is the earthquake magnitude determined by Japan Meteorological Agency, *D* is a focal depth (km), *X* is the shortest distance from a source fault to an estimation point (km). The earthquakes that occur around an OBS are defined as the hypothetical earthquakes whose epicenters are included within 30 km east or west and/or 90 km north or south of the OBS.

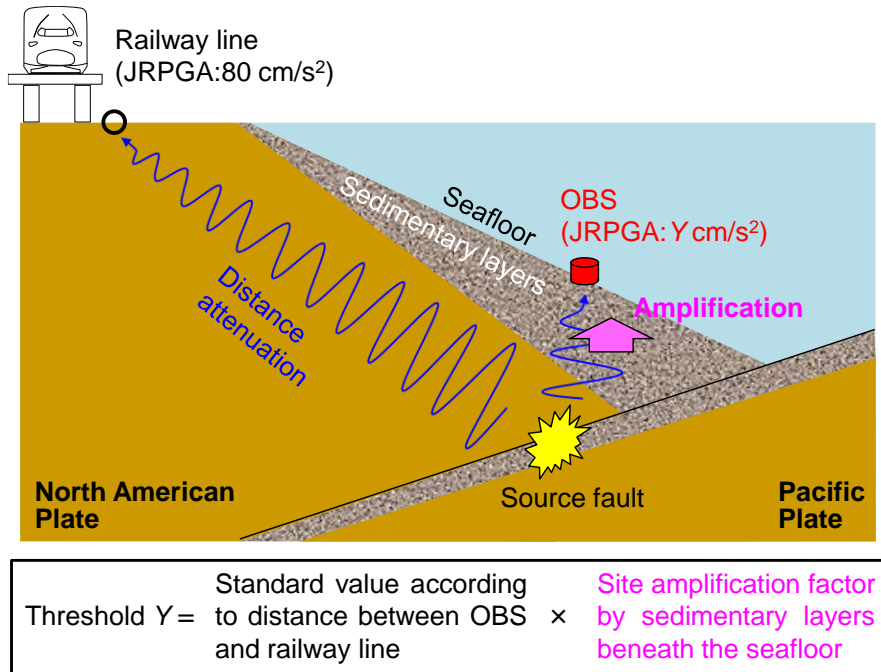


Figure 2: The conceptual figure showing the conditions for setting the threshold for each OBS.

A site amplification factor generally has a different value for each observation point depending on the hardness and thickness of the sediment beneath the observation point. Due to little information about the hardness and thickness of the sedimentary layers beneath the seafloor, the site amplification factor (*amp*) is empirically evaluated as the ratio of the observed value by the OBS to the estimated value by the attenuation relation in equation (1) [4,5], which is expressed by the following equation.

$$amp = \frac{JRPGA \text{ observed by OBS}}{JRPGA \text{ estimated by distance attenuation relationship}} \quad (2)$$

The earthquakes used in the calculation by equation (2) are the actual earthquakes whose epicenters are included within 30 km east or west and/or 90 km north or south of the OBS. Because there were not many records of S-net and it was not possible to evaluate the site amplification factor for each OBS as of 2017, the common site amplification factor for all OBS was provisionally evaluated as the average value by 47 records from 36 earthquakes observed from June 2016 to April 2017. In Figure 3, histogram of site amplification factors as of 2017 is shown.

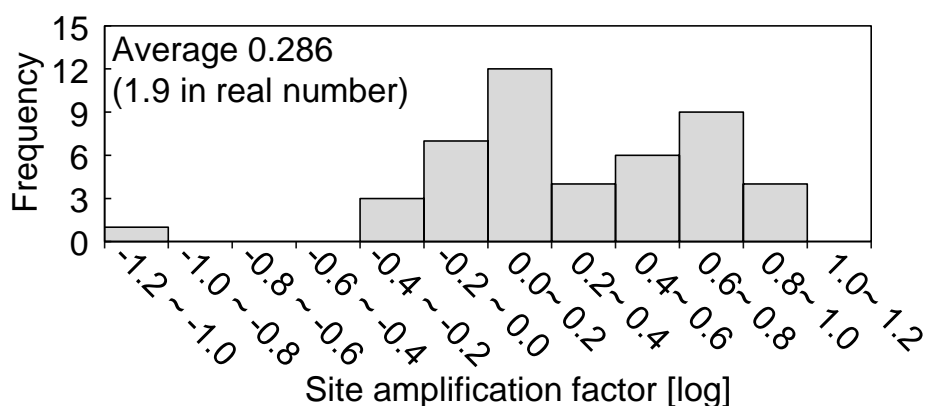


Figure 3: Histogram of site amplification factors as of 2017.

### 3 Effect of sediment thickness beneath the seafloor on site amplification factor

We verified the effect of the amplification by sedimentary layers beneath the seafloor on the site amplification factor evaluated from equation (1) and (2) using the accumulated data of S-net [9]. The data used for verification were 4,592 records from 360 earthquakes whose JMA magnitude over 4.5 observed from March 2016 to April 2020 by the OBSs of S-net. Because the thicker the sedimentary layer, the more earthquake motion is generally amplified, and we decided to evaluate the relationship between the sedimentary layer thickness and the site amplification factor in this study. The thickness of the sedimentary layer beneath the seafloors estimated by measuring the distance from the seafloor to the deepest reflecting surface using the cross sections from multi-channel seismic reflection survey (MCS) obtained in previous studies [10, 11]. In Figure 4, the estimated thicknesses of the sedimentary layer beneath the OBSs of S-net excluding S6 are shown.

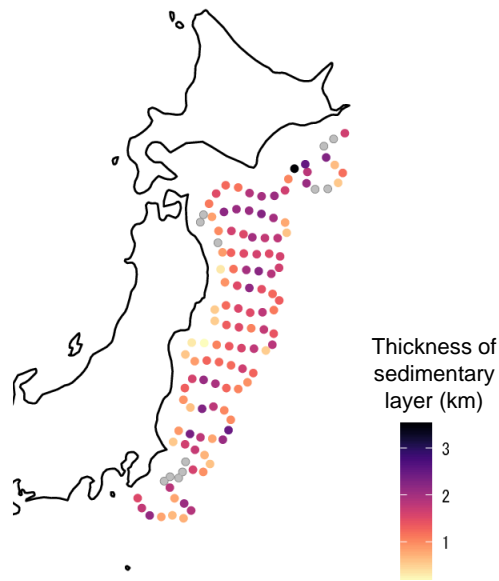


Figure 4: The estimated thicknesses of the sedimentary layer beneath the OBSs of S-net excluding S6.

In Chapter 2, the earthquakes used in evaluation of the site amplification factors were limited to the earthquakes with the epicenters included within 30 km east or west and/or 90 km north or south of the OBS. In order to easily confirm the effect of using only nearby earthquakes, we evaluated the relationship between the sediment thicknesses and the site amplification factors when using only earthquakes with epicenters within 45 km from the OBS and when using all earthquakes. In Figure 5, the relationship between the sediment thicknesses and site amplification factors are shown. The logarithmic correlation coefficient between the sediment thicknesses and the site amplification factors was approximately 0.2, confirming a weak positive correlation, as shown in Figure 5. By individually re-evaluating the site amplification factor, which has been currently common in all OBSs, the evaluation accuracy of the factor will be improved because the sediment layer thickness was unique for each OBS as shown in Figure 4. Since there was, however, large variation in site amplification factors depending on the records, further improvement of evaluation accuracy will be required in the future. The logarithmic correlation coefficient between site amplification factors and sedimentary layer thicknesses was higher when all earthquakes were used than when only earthquakes whose epicenters were within 45 km from the OBS were used: therefore, we decided to use all earthquakes, not just nearby earthquakes, in evaluating the site amplification factor.

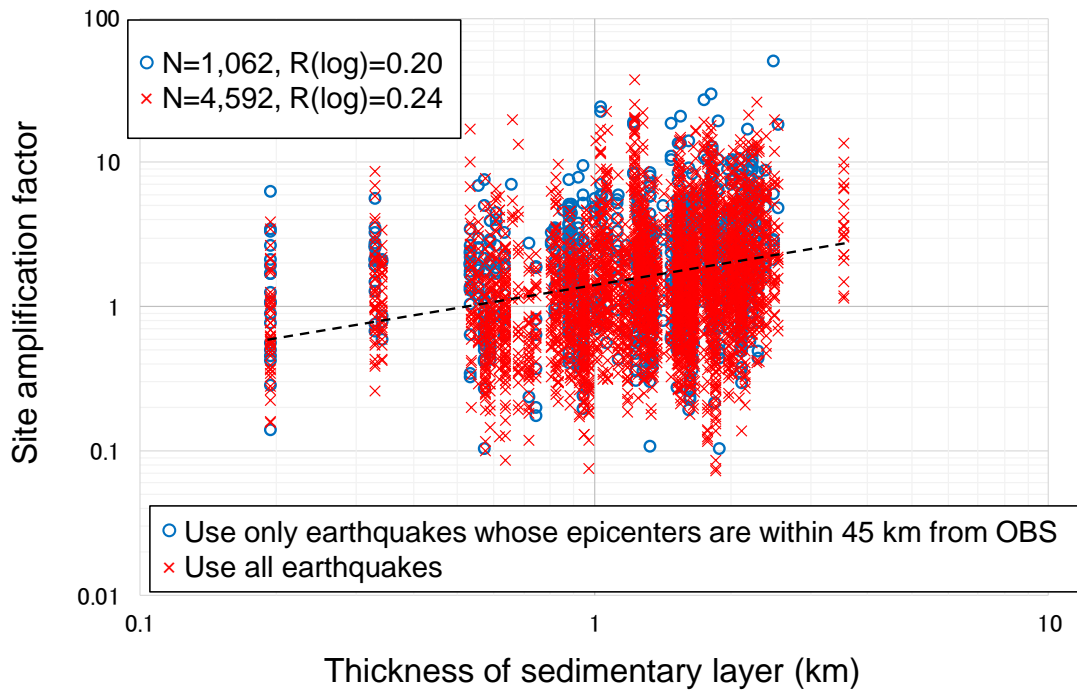


Figure 5: Relationship between sediment thicknesses and site amplification factors, where  $N$  is the number of data,  $R(\log)$  is the logarithmic correlation coefficient.

#### 4 Evaluation of site amplification factors for each OBS based on accumulated data

We evaluated the site amplification factor for each OBS using the further accumulated OBS data, which consisted of 34,839 records from 474 earthquakes whose magnitude over 4.5 from March 2016 to May 2022 [9]. In Figure 6, histogram of the magnitudes of the earthquakes used for evaluating the site amplification factors of the OBSs of S-net is shown. As shown in Figure 6, the majority of earthquakes used in the evaluation are earthquakes with a magnitude of 5 or less: therefore, there are likely to be few records that include the effects of soil nonlinearity during strong earthquakes.

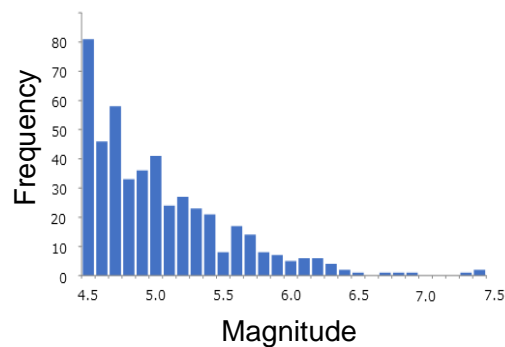


Figure 6: Histogram of the magnitudes of the earthquakes used for evaluating the site amplification factors of the OBSs of S-net.

In Figure 7, the site amplification factors calculated by equation (1) and (2) and their logarithmic average values for each OBS are shown. The logarithmic average value for each OBS showed a unique value, as shown in Figure 7. The logarithmic average site amplification factor for all the OBS was 2.09, which was almost the same as the current value of 1.9: therefore, the current common site amplification factor was generally reasonable on average. The OBS whose site amplification factor was lower than the current value of 1.9 may not have been able to issue EEWs for earthquakes that should have been issued in the past. Conversely, the OBS whose site amplification factor was higher than the current value of 1.9 may have previously issued warnings for earthquakes that did not require an early earthquake warning. By precisely determining the site amplification factor for each OBS and utilizing those factors, missed or excessive warnings will be expected to be prevented.

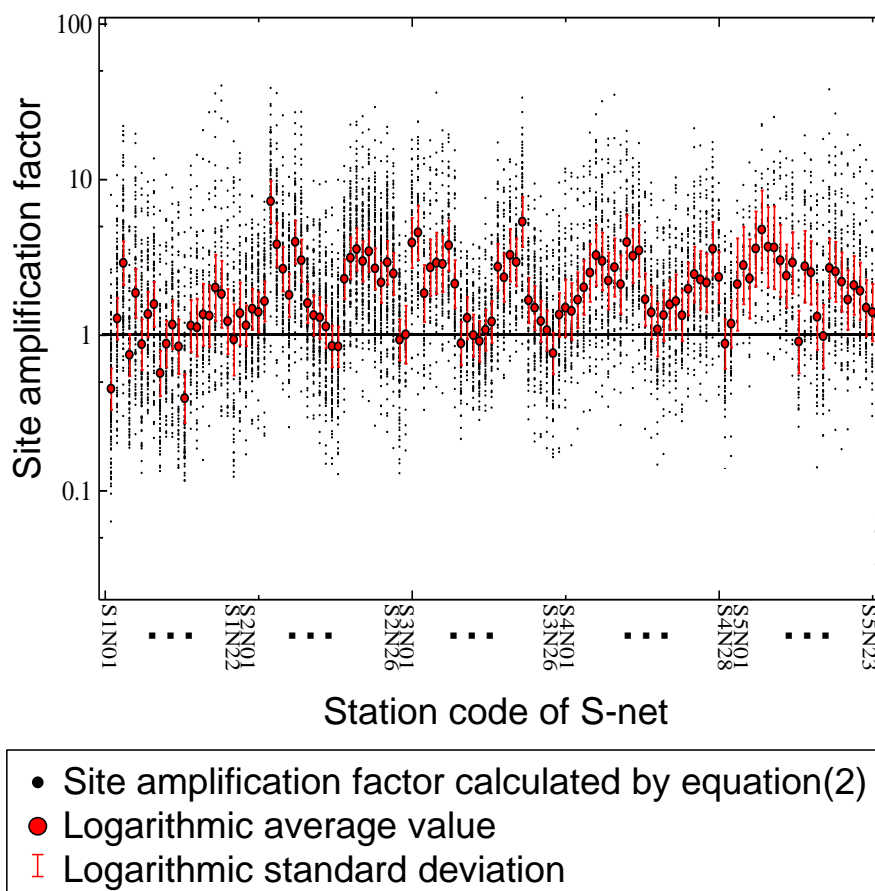


Figure 7: Site amplification factor for each OBS

## 5 Conclusions and Contributions

In this study, we evaluated the site amplification factor of at the seafloor, which has been common value for all the OBS in JR East's EEW system, using accumulated data observed by the OBS of S-net, in order to improve the accuracy of EEWs for railways. The site amplification factors evaluated in this study was correlated with the sediment

thicknesses beneath the seafloor: therefore, the number of missed and excessive warnings will be expected to be reduced by utilizing those factors.

## Acknowledgements

This study is joint research with Japan Agency for Marine Earth Science and Technology (JAMSTEC), NIED, and Railway Technical Research Institute (RTRI). We thank JAMSTEC and NIED to provide us with information on seabed ground information [10, 11].

## References

- [1] K. Mizuno, A. Takizawa, J. Oonuki, H. Osawa, "Detection of increasingly severe natural phenomena and disaster prevention for railway facilities", JR EAST Technical Review, 35, 31-36, 2017.
- [2] T. Kanazawa, K. Uehira, M. Mochizuki, T. Shinbo, H. Fujimoto, S. Noguchi, T. Kunugi, K. Shiomi, S. Aoi, T. Matsumoto, S. Sekiguchi, Y. Okada, "S-net project, cabled observation network for earthquakes and tsunamis", SubOptic 2016, WE2B-3, 2016.
- [3] S. Aoi, Y. Asano, T. Kunugi, T. Kimura, K. Uehira, N. Takahashi, H. Ueda, K. Shiomi, T. Matsumoto, H. Fujiwara, "MOWLAS: NIED observation network for earthquake, tsunami and volcano", Earth, Planets and Space, 72, 126, 2020, <https://doi.org/10.1186/s40623-020-01250-x>.
- [4] H. Miyakoshi, H. Suzuki, S. Yamamoto, W. Suzuki, S. Aoi, "Earthquake early warning for Shinkansen using ocean bottom seismometer", "Congress Proceedings of 12<sup>th</sup> World Conference on Railway Research", IP06-4, 1-6, 2019.
- [5] H. Suzuki, H. Miyakoshi, S. Yamamoto, M. Korenaga, W. Suzuki, S. Aoi, "Earthquake early warning for Shinkansen utilizing ocean bottom seismometer and its effect", Journal of Japan Society for Natural Disaster Science, 40, 191-206, 2021 (in Japanese with English abstract).
- [6] Y. Nakamura, "Earthquake warning system in Japan National Railways", Railway Technology, 42, 371-376, 1985 (in Japanese).
- [7] Y. Bito, Y. Nakamura, K. Tomita, "On a method of reporting the train service after an earthquake for the Tokaido-Sanyo Shinkansen", Railway Technical Research Report, Vol. 1294, pp. 1-38, 1985 (in Japanese with English abstract).
- [8] M. Korenaga, N. Iwata, S. Yamamoto, S. Noda, S. Shimono, T. Ono, "Proposal of attenuation relations for use of earthquake early information", Proceedings of JSCE 2011 Annual Meeting, I-481, 961-962, 2011 (in Japanese).
- [9] National Research Institute for Earth Science and Disaster Resilience, NIED S-net, National Research Institute for Earth Science and Disaster Resilience, 2019, DOI:10.17598/NIED.0007.
- [10] JAMSTEC, "JAMSTEC Seismic Survey Database", JAMSTEC, 2004, DOI:10.17596/0002069.



- [11] A. Nishizawa, K. Uehira, M. Mochizuki, "Sediment distribution beneath S-net stations derived from multi-channel seismic reflection profiles and hypocenter determination using the sediment correction", Technical Note of the National Research Institute for Earth Science and Disaster Resilience, 471, 1-18, 2022 (in Japanese with English abstract).